Available online at www.sciencedirect.com
ScienceDirect
Journal of Power Sources 159 (2006) 543–559
JOURNAL OF POWER SOURCES
www.elsevier.com/locate/jpowsour

Modeling solid oxide fuel cell operation: Approaches, techniques and results

Roberto Bove [a,*], Stefano Ubertini [b]

[a] *Industrial Engineering Department, University of Perugia, Italy*
[b] *Mechanical Engineering Department, University of Rome "Tor Vergata", Italy*

Received 25 August 2005; received in revised form 20 October 2005; accepted 9 November 2005
Available online 20 December 2005

Abstract

In the present paper, a three-dimensional, time-dependent SOFC numerical model is defined, considering all the phenomena occurring in each component of the fuel cell. All the equations are written in a partial differential form, thus the model is independent from the cell geometry (planar, tubular, monolithic) and the modeling approach (i.e. time-dependent, 3D, 2D). The triple-phase-boundary (TPB) is modeled as a finite region, as well as a non-dimensional interface area. In the latter case the source terms of the energy, mass and electrical conservation equations are treated as a boundary conditions. Finally, a literature review is conducted. Some results from the models previously developed by the authors or found in the literature survey are presented. Each of them can be reviewed as a simplified version of the model presented in the present paper. The simplified assumptions and the related omissions that each of those approaches imply are also analyzed.

Keywords: Solid oxide fuel cell modeling; Modeling approaches; SOFC analysis

1. Introduction

Solid oxide fuel cells (SOFCs) are considered promising energy conversion devices thanks to their several potential benefits, including low pollutant emissions, high-energy efficiency, the possibility of using different kinds of fuels and the possibility to build CHP and hybrid systems.

However, SOFC technology is still in embryonic infancy and many problems (i.e. mechanical stress, electrode sintering, electrode and interconnect materials and fabrication, startup time) must be solved in order to achieve the goal of a highly efficient and clean energy system with at least the same reliability, costs and lifetime of the "traditional" energy systems.

This challenge entails an increased research effort for industry and research institutions in order to develop advanced numerical models and computer codes, that can be used in both industrial and research environments for fuel cells design and development. This could yield a better understanding of the physical processes and help fuel cell designers to define more promising strategies.

The performance, the reliability and the duration of an SOFC is directly related to the processes that occur within the cell. The control of these processes requires primarily an understanding of SOFC physics and chemistry as well as the capability to modify one or more interdependent processes parameters in a given direction. This task is made even more difficult by the complexity and the vast number of physical and chemical processes that occur simultaneously in an SOFC and/or in an energy system based on SOFCs. All this along with the high number of parameters involved necessarily make computer models attractive for their potential of modeling physical fluid phenomena that cannot be easily measured.

Enormous progress has been made in the last decade on numerical, analytical and computational tools for SOFCs. One of the first significant publications on SOFC modeling is Bossel's [1], published in 1992 as a result of an Electric Power Research Institute (EPRI) project. The analysis assesses the main differences, in terms of performance, among different SOFC configurations, using the same materials characteristic. The model is quite simple, but at the same time provides a very important tool to investigate cross-plane and in-plane resistance. The SOFC

* Corresponding author. Tel.: +39 075 585 3747; fax: +39 075 585 3736.
E-mail address: rbove@unipg.it (R. Bove).

0378-7753/$ – see front matter © 2005 Elsevier B.V. All rights reserved.
doi:10.1016/j.jpowsour.2005.11.045

configurations studied at that time still constitutes the main geometrical design and the results of that study still represent a relevant base point for understanding the performance potential of any SOFC configuration. The model developed by Achenbach [2], instead, is based on a three-dimensional and time-dependent approach for planar solid oxide fuel cell simulation. This model appears to be quite accurate, and uses differential and finite equations that allow detecting gas concentration, current density, temperature variation within the cell, along with the effects of different fuels, flow manifolding and of three-dimensional phenomena. The model considers the effect of ohmic losses and anode and cathode polarizations, in the form of "activation" polarization.

The approach used by Bessette et al. [3] for a tubular solid oxide fuel cell model, is similar to Achenbach's. Besides the ohmic and activation losses, a method to evaluate concentration polarization is given. The results show the fuel cell local characteristics for different axial and angular positions. Moreover, the effects of different oxidants and fuels are shown.

Several other publications can be found in the literature, which illustrate more accurate models, thanks to the enhanced computational performance. Examples of very detailed models are provided by Ferguson [4] or Petruzzi et al. [5].

However, considerable work is still necessary in developing and testing sub-models to describe unresolved individual physical processes that, especially for the porous electrodes, introduce an excess of empiricism into computation.

Numerical modeling is now playing an important role and represents a critical aspect of the technology development process in industry. This is mainly due to the increase in competition in all fields of engineering and to the enormous improvements in computer technology in the last two decades. Moreover, modeling is widely utilized within industry because it is a valid tool to investigate physical fluid systems more cost effectively and more rapidly than with experimental procedures. In particular, the process of modeling is integrated into the entire engineering process that usually foresees a combined experimental–numerical approach:

- numerical simulations are necessary to have direct "insight" into the system and to allow studying different components design, stack and cell configurations and layouts, fuels, etc. and to determine optimum operating conditions; this reduces the number of experimental tests to be performed and the costly and time consuming physical prototyping; in brief, three roles can be identified for numerical modeling: interpretation, design and prediction;
- measurements are necessary to validate numerical models and to make the final choice among those few configurations selected through computational simulations.

However, numerical modeling must be used very carefully, especially when it is used for prediction purposes. It must be borne in mind that numerical modeling means reproducing the behavior of a system by solving a set of equations describing the evolution of variables that define the state of the system. This evolution is governed by processes that are extremely complex and some of them are completely unknown. This means that even with a high level of model complexity, models are only a simplified representation of real physics. Therefore, the accurate prediction of actual performances cannot be guaranteed and is instead very difficult even after appropriate validation of the models.

The present paper is organized in order to follow the usual steps in the development of a numerical model:

- understanding the physical system and translating it into mathematical equations; in their most general form, these are usually a set of partial differential equations (mathematical model);
- these equations cannot be usually analytically solved and are discretized to allow numerical solution; spatial domain is divided into small elements constituting the grid or mesh (numerical model);
- after generating a reasonably fine numerical grid on which the discrete algebraic equations will be solved, a set of problem-dependent boundary and initial conditions are specified (boundary conditions);
- it is then shown how the complete, 3D and time-dependent problem can be simplified, according to the specific needs, to steady state conditions, 2D, 1D and 0D;
- once a computational model has been developed for a particular application, the results must be compared with physical reality; this validates the code and avoids blind acceptance of numerical results, which is often a problem with commercial software use (validation);
- some results obtained by the authors in previous studies, as well as simplified applications of the model are shown (results).

2. Mathematical model

A comprehensive analysis of solid oxide fuel cells (SOFC) phenomena requires an effective multidisciplinary approach. Chemical reactions, electrical conduction, ionic conduction and heat transfer take place all at the same time and are tightly coupled.

SOFC can be manufactured in different geometrical configurations, i.e. planar, tubular or monolithic.

Regardless of the geometrical configuration, a solid oxide fuel cell is always composed of two porous electrodes (anode and cathode), a dense electrolyte, an anodic and a cathodic gas channel and two current collectors. For sake of simplicity, in Fig. 1, the planar configuration is taken as reference. It is interesting to note that for the flat planar configuration (Fig. 1), the current collector acts also as a gas channel, while for the tubular and monolithic, one electrode acts as the gas distributor.

The task of the gas channel is to guide the gas on the electrode surface for enabling a uniform distribution. If the cell operates on a hydrocarbon, rather than on hydrogen, the reforming reaction (1) takes place in the anodic gas channel:

$$C_nH_mO_p + (n - p)H_2O = nCO + (n - p + m/2)H_2 \quad (1)$$

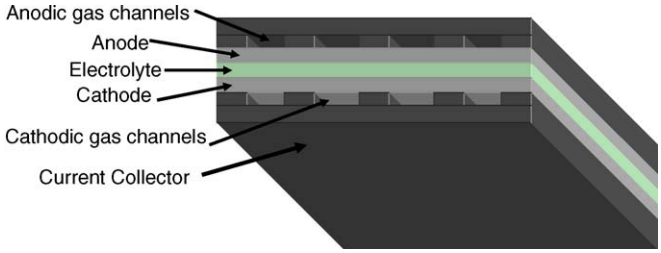

Fig. 1. Schematic representation of a flat planar SOFC.

Furthermore, carbon monoxide reacts with water to generate additional hydrogen and carbon dioxide:

$$CO + H_2O \leftrightarrow CO_2 + H_2 \quad (2)$$

Since the anode is porous, the gases in the anodic gas channel permeate it. The hydrogen generated from reactions (1) and (2) reacts with the oxygen ions coming from the cathode through the electrolyte, thus generating water:

$$H_2 + O^{2-} \rightarrow H_2O + 2e^- \quad (3)$$

The water produced goes back to the anode channel and exits the cell, together with the other unoxidized gas species. The result for the anodic side is a hydrogen flux from the channel to the anode–electrolyte interface and a water flux on the opposite path.

At the cathode side, instead, oxygen in the cathodic channel permeates the cathode where ions form and migrate through the electrolyte:

$$\frac{1}{2}O_2 + 2e^- \rightarrow O^{2-} \quad (4)$$

The result for the cathode is a one way flux from the channel to the electrode–electrolyte interface (Fig. 2).

The electrons released from Eq. (3) flow from the reaction zone (typically very close to the anode/electrolyte interface) to the current collector, through the anode. At the cathode side, these electrons flow from the current collector to the cathodic reaction zone, where reaction (4) takes place.

Heat is generated inside the cell by the following heat sources:

- Electrochemical reactions (3) and (4), taking place very close to the electrode–electrolyte interface (i.e. at the so-called triple-phase-boundary (TPB)) generate heat, due to the entropy increase.
- Chemical reactions (1) and (2), taking place in the anodic gas channel if hydrocarbons are internally reformed. The steam reforming reaction (1) is endothermic, thus heat is absorbed from the surroundings.
- Ohmic resistance; the ionic and electronic currents, when passing through the electrolyte and the electrodes, generate the so-called Joule heating.
- Activation over-potential due to the activation energy; the current flow generates an electrochemical loss that is translated into a heat source.

The heat generated inside the cell is removed by the incoming anodic and cathodic gases. The heat transfer between the cell components, the gases and the surroundings, acts for conduction, convection and radiation.

In the following, the mathematical model of each component is defined, thus obtaining the system of equations that analytically describes a generic SOFC. Furthermore, the completion of the model with the boundary conditions is discussed.

2.1. Channels flow

Using an Eulerian approach, the description of fluid motion requires the determination of the thermodynamic state, in terms of sensible fluid properties, pressure, P, density, ρ and temperature, T, and of the velocity field $\vec{u}(\vec{x}, t)$ [6–10].

Therefore, in a three-dimensional space for a given thermodynamic system having two intensive degrees of freedom, we have six independent variables as unknowns of the so-called "thermo-fluid dynamic problem", thus requiring six independent equations. The six equations are given by the equation of state and the three fundamental principles of conservation:

- equation of state for involved gas species;
- mass continuity; actually, if a mixture of gases is present, species mass fractions are additional unknowns, thus requiring the mass conservation equation for each specie;
- Newton second law or momentum equation (three equations in a three-dimensional space x, y and z);
- energy conservation (First law of thermodynamics).

Since gases in SOFCs are far from the critic conditions, perfect gas equation of state is usually employed:

$$P = \rho RT \quad (5)$$

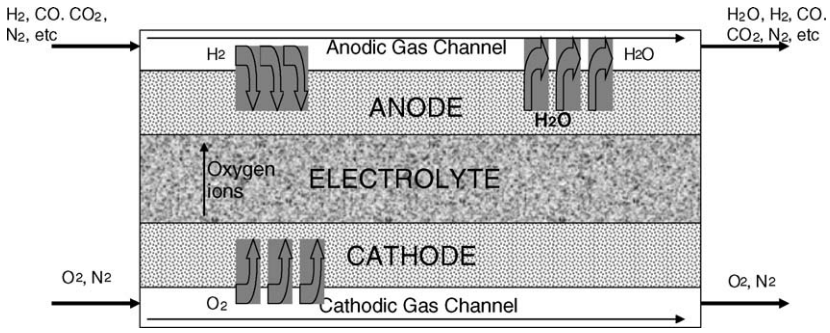

Fig. 2. Gas fluxes inside the SOFC.

where P is the gas pressure, ρ the density, R the universal gas constant and T is the temperature.

The conservation equations can be expressed in either a differential or integral form. The differential form, usually called primitive formulation, is the most used in fluid mechanics, and is used in the present formulation.

Considering that the working fluid in the gas channels of an SOFC is a reacting mixture of gases, mass conservation can be analytically described by the following transportation equation:

$$\frac{\partial \rho Y_i}{\partial t} + \vec{u} \cdot \vec{\nabla}(\rho Y_i) = \nabla \vec{m}_i + \omega_i \tag{6}$$

where i denotes the generic ith specie, ω_i the rate of production or consumption of the specie, $\vec{m}_i$ the mass diffusion flux, Y_i the mass fraction of the ith species, and $\vec{u}$ is the gas velocity. According to Fick's law of binary diffusion, the ith specie diffusion flux can be read as follows:

$$\vec{m}_i = \left| \rho D_i \vec{\nabla}(Y_i) \right| \tag{7}$$

where D_i is the mass diffusion coefficient.

The overall fluid density is the sum $\rho = \sum_{i=1}^{N_s} Y_i \rho$ over all species and leads to the standard continuity equation:

$$\frac{\partial \rho}{\partial t} + \nabla(\rho \vec{u}) = \omega \tag{8}$$

where ω is a source term that takes into account mass variation due to the electrochemical reaction.

In order to calculate the physical properties of the multicomponent mixture, including viscosity, specific heats at constant volume and at constant pressure and laminar thermal conductivity, the assumption that the components form an ideal mixture is usually made. An arbitrary constitutive fluid property may be calculated from the property value for the fluid ith component through the following equation:

$$x = \sum_i x_i Y_i \tag{9}$$

Regarding the momentum conservation, the Navier–Stokes equations, governing unsteady compressible viscous flows, are the basis for all models. However, the thermal and chemically reacting flows through SOFC gas channels are often characterized by relatively slow flow motion, much slower than the speed of sound, and by partially varying mixture density. Variations of the density are caused in these cases either internally by heat release of chemical reactions or externally by wall heating and by mass variation due to the electrochemical reaction but not by compression of the gas. This situation is characterized by a low Mach number, (near the incompressible limit) and is consequently modeled by a scale analysis of the Navier–Stokes momentum equations with respect to small Mach numbers:

$$\frac{\partial \vec{u}}{\partial t} + \vec{u} \nabla \vec{u} = -\vec{\nabla} P + \frac{\mu}{\rho} \nabla^2 \vec{u} + \vec{f} \tag{10}$$

where $\vec{f}$ is a specific prescribed body force (i.e. gravity force) and μ is the fluid dynamic viscosity. The system of equations should still be supplemented by the laws of dependence of viscosity and thermal conductivity on the fluid state. However, in many situations they are assumed to be constant.

In the above formulation of the governing equations, the velocity field and the pressure field are treated as unknowns in the fluid domain.

It is important to notice that the general equations of fluid motion are independent of the coordinate system. Therefore, Eq. (10), given in the Cartesian coordinate system, can be converted and used with a specific coordinate system orientation relative to the flow field (i.e. tubular SOFC).

If the divergence of Eq. (10) is taken, the pressure field can be calculated as a solution of Poisson's equation:

$$\nabla^2 P = -\nabla(\vec{u} \nabla \vec{u}). \tag{11}$$

The physics of laminar and turbulent incompressible flows are well represented by the above formulation of the Navier–Stokes equations. Closure of this system of equations is a non-trivial task and closed solutions are available only for exceptional cases. Considering that the gas speed in SOFC gas channels is always very low, it is a common practice to assume a laminar flow [11].

This assumption significantly reduces the computational cost and allows to quickly determine the velocity profile and the pressure drop through the channel, $\Delta P \propto \rho u_m^2/2$, being u_m the average channel velocity.

Temperature profiles inside the cell can be obtained through the energy equation, which can be written in numerous but equivalent forms. Indicating with e the fluid energy per unit mass, the following equation for the conservation of energy is derived:

$$\rho \frac{\partial e}{\partial t} + \rho \vec{u} \cdot \vec{\nabla} e = \nabla \vec{Q} + S_q \tag{12}$$

where S_q is the volumetric heat source term and $\vec{Q}$ is the heat flux vector only from conduction, which, according to Fourier's law, can be related to the temperature field:

$$\vec{Q} = -\lambda \vec{\nabla} T \tag{13}$$

where λ is the thermal conductivity coefficient.

The fluid energy per unit mass, in its most general form, is the sum of the specific internal energy and the specific kinetic energy:

$$e = c_v T + \frac{u^2}{2} + \vec{g} \cdot \vec{r} \tag{14}$$

where c_v is the specific heat at constant volume, $\vec{g}$ the gravity acceleration and $\vec{r}$ is the unity gravity vector.

Considering that the working fluid is a mixture of gases, the potential energy, $\vec{g} \cdot \vec{r}$ and the kinetic energy, $u^2/2$, are usually neglected and the fluid energy per unit mass coincides with the specific internal energy.

The heat source term S_q in Eq. (12) incorporates the viscous dissipation (always positive) and the heat generated or absorbed by the chemical reactions (i.e. shift and reforming reactions). Furthermore, the convective thermal flux at the boundaries and the radiative heat transfer with solid cell components must be considered (boundary or interface source terms).

In any multicomponent system involving chemical reactions, mass and energy source terms must be considered in order to solve the thermo-fluid dynamics problem. These reactions can be written in the following form:

$$\sum_{i=1}^{N_s} r_{ik} c_i \Leftrightarrow \sum_{i=1}^{N_s} p_{ik} c_i \quad k = 1, N_r \tag{15}$$

where N_r is the number of reactions, N_s the number of species, r_{ik} and p_{ik} the stoichiometric coefficient of the reactants and the products of the kth reaction and c_i is the chemical of the ith specie. Knowing the reaction rates of the forward and the backward reactions (i.e. Arrhenius equation), the source term ω_i in the species transport Eqs. (6) can be calculated. Moreover, each reaction is characterized by an absorption (endothermic) or a release (exothermic) of heat, which allows to determinate the chemical source term in the energy equation.

Regarding the gas channels of an SOFC, significant chemical reactions may take place only in the anode gas channel: the reforming reaction (1) and the shift reaction (2). The shift reaction is a fast process and is usually assumed to be in equilibrium. The steam reforming process instead is much slower, thus the kinetic of the reaction needs to be considered.

2.2. Electrodes

To solve the electrical problem, two variables need to be found, i.e. the electrical potential (scalar) and the current density (vector). Fig. 3 represents the anode schematically. SOFC electrodes are typically made of mixed electronic and ionic conducting materials [12], thus both electrons and ions can flow through them. Regarding the anode (Fig. 3), ions coming from the electrolyte flow through the anode, thus combining with H_2 and releasing electrons at the so-called triple-phase-boundary (TPB) zone. Consequently, electrons, flow towards the anodic current collector. The electrical problem is solved with one vector and one scalar relationship.

The vector relationship is given by Ohm's law:

$$\vec{J} = -\sigma \vec{\nabla} \phi \tag{16}$$

where $\vec{J}$, σ and ϕ are, respectively, current density, conductivity and electrical potential, and can be referred to either the ionic or the electronic current. The scalar relation is provided by the current conservation:

$$\frac{\partial \rho_e}{\partial t} + \vec{\nabla} \cdot \vec{J} = \begin{cases} j & \text{in the TPB} \\ 0 & \text{elsewhere} \end{cases} \tag{17}$$

where ρ_e is the electronic or ionic charge density, and j is the current generation rate, produced at the three-phase-boundary. Since the cell charging time is very short, compared to the other phenomena acting in the fuel cell [13], this can be considered at steady state, i.e. the first term on the left hand side of Eq. (17) can be neglected.

The current source is regulated by the Bultler–Volmer equation:

$$j = j_0 \left[\exp\left(\frac{\alpha_1 \eta_{act}}{RT}\right) - \exp\left(\frac{\alpha_2 \eta_{act}}{RT}\right) \right] \tag{18}$$

In expression (18) j_0 is the exchange current density and depends on the electrode properties and operation, α_1 and α_2 are two transfer coefficients, and η_{act} represents the latter. The activation loss can quantified as:

$$\eta_{act} = V_{rev} - \left| \phi_{electrode} - \phi_{electrolyte} \right| \tag{19}$$

where V_{rev} is the reversible potential between the electrode and the electrolyte, and can be computed with Nernst's equation.

Since the TPB boundary is usually very small, compared to the electrode and electrolyte thickness, the current generation is sometimes considered to take place at the electrode–electrolyte boundary [4,14,15], thus Eq. (18) is considered a boundary condition for Eq. (17) with no source term, and the term j_0 takes into account that only a part of the interface is active in the reaction, as explained in Section 4.

Combining Eqs. (16) and (17), the following relationship is obtained:

$$\nabla^2 \phi = \begin{cases} -\dfrac{j}{\sigma} & \text{in the TPB} \\ 0 & \text{elsewhere} \end{cases} \tag{20}$$

It is interesting to observe that, due to the solid state of the entire cell, and due to the non-perfect planarity of the components, the so-called contact resistance is generated at the electrode/electrolyte interface and at the electrode/current collector interface. Although it is difficult to yield a theoretical formulation for this loss, experimental or empirical data can be given as an additional boundary condition.

Considering the porous media as continuum, the energy equation can be written as:

$$c \frac{\partial T}{\partial t} + \nabla \vec{Q} + S_q = 0 \tag{21}$$

where T and c are the temperature and the specific heat of the medium, respectively, and Q has already been defined (Eq. (13)). The source term represents the heat generated due to:

1. Joule effect, due to the ohmic resistance.
2. Reversible heat, associated to chemical reactions (3) or (4).
3. Activation loss.

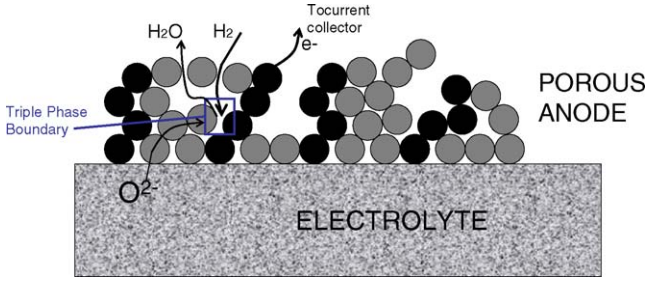

Fig. 3. Triple-phase-boundary (TPB) and anodic reaction.

While the Joule effect takes place in all the electrode domain, the last two heat sources are localized in the TPB.

$$S_q = \begin{cases} \sigma\vec{\nabla}\phi\cdot\vec{\nabla}\phi + \dfrac{J}{2F}T\Delta S + J\eta_{act} & \text{in the TPB} \\ \sigma\vec{\nabla}\phi\cdot\vec{\nabla}\phi & \text{elsewhere} \end{cases} \quad (22)$$

In expression (22), ΔS is the entropy change associated with either reaction (3) or reaction (4).

Similarly to Eqs. (17) and (18), if the reaction is considered at the electrode/electrolyte interface, Eq. (22) becomes a boundary condition:

$$S_q = \sigma\vec{\nabla}\phi\cdot\vec{\nabla}\phi \quad (23)$$

The heat generation is considered as a boundary condition at the electrode/electrolyte interface.

Due to the structure of the electrodes, the velocity, pressure and species distribution needs to be studied using the theory of mass transport in porous media. This topic has been extensively studied over the years, and reported in the open literature. Examples of detailed studies are given by Bird et al. [10], Froment and Bishoff [16], Bear and Buchlin [17], and Bear [18].

The mass transport equation needs to take into account the effect of the medium porosity. Moreover, the molar flux is mainly due to convection in the gas channel, whereas in the porous media, diffusion is the main cause. The general form for the mass transport equation is [19]:

$$\frac{\varepsilon}{RT}\frac{\partial(X_i P)}{\partial t} = -\nabla\vec{N}_i + \omega_i \quad (24)$$

where ε represents the porosity of the electrode, X_i the mole fraction and N_i the mole flux of the ith species. The reaction rate is given by the following expression:

$$\omega_i = \begin{cases} \dfrac{j}{2F} & \text{in the TPB} \\ 0 & \text{elsewhere} \end{cases} \quad (25)$$

In expression (25), F is Faraday constant, and j is defined in expression (18). As for the electrical problem, if the reaction zone is reduced to the electrode–electrolyte interface, the reaction rate is zero in all the electrode, and the mass flux is given as a boundary condition.

A well established way of describing the diffusion phenomenon in the SOFC electrodes is through either the Fick's law [20–24], or the Stefan–Maxwell equation [25–28]. Some authors use more complex models, like for example the dusty-gas model [29] or derived from it [30,31]. A comparison between the three approaches is reported by Suwanwarangkul et al. [19], who concluded that the choice of the most appropriate model is very case-sensitive, and should be selected, according to the specific case under study.

If Fick's law is considered, the mass flux is given by the following expression [19]:

$$N_i = -\frac{D_{i,\text{eff}}}{RT}\frac{\partial(X_i P)}{\partial z} \quad (26)$$

where z is the direction of the electrode thickness.

The diffusion coefficients ($D_{i,\text{eff}}$) are modified to take into account the interaction with the pore walls. The Bruggemann correction allows the evaluation of these coefficients, through the following expression [17]:

$$D_{i,\text{eff}} = \varepsilon^{\tau} D_i \quad (27)$$

where τ is the tortuosity of the porous medium, D_i the ordinary diffusion coefficient and $D_{i,\text{eff}}$ is the diffusion coefficient in the porous medium. Some authors, e.g. [20,21,27], instead, use the following expression:

$$D_{i,\text{eff}} = \frac{\varepsilon}{\tau} D_i \quad (28)$$

When the Stefan–Maxwell expression is used, the diffusion of each gas species is linked to the other species composing the gas mixture [19]:

$$\sum_{j=1,\, j\neq i}^{n} \frac{X_j N_i - X_i N_j}{D_{ij,\text{eff}}} = -\frac{P}{RT}\frac{\mathrm{d}X_i}{\mathrm{d}z} \quad (29)$$

with n indicating the number of gas mixture components, and $D_{ij,\text{eff}}$ the effective binary diffusion coefficient.

A more elaborated expression, that takes into account the Knudsen diffusion, is given by the dusty-gas model:

$$\frac{N_i}{D_{ik,\text{eff}}} + \sum_{j=1,\, j\neq i}^{n} \frac{X_j N_i - X_i N_j}{D_{ij,\text{eff}}} = -\frac{P}{RT}\left(\frac{\mathrm{d}X_i}{\mathrm{d}z}\right) \quad (30)$$

where $D_{ik,\text{eff}}$ indicates the effective Knudsen diffusion coefficient (Veldsink et al. [29]).

The momentum equation inside the porous media is provided by Darcy's law:

$$\vec{u} = -\frac{k}{\eta}\vec{\nabla}P \quad (31)$$

where k is the permeability of the porous media, and η is the dynamic viscosity.

2.3. Current collectors

Phenomena acting in the current collectors are intrinsically easier than those occurring in the other parts of the fuel cell. In this component, in fact, only electrons flow, thus requiring only the equations needed for modeling the electrical problem and the temperature distribution. Considering that the current collectors are usually made of very high conductive materials, the relative ohmic resistance, depending on the model purpose, is usually ignored. As a consequence, even the heat generation, that is due only to the Joule effect, can be ignored.

Regarding the electrical problem, Eq. (20) is simplified for the current collector as:

$$\nabla^2\phi = 0 \quad (32)$$

The current distribution can be obtained by:

$$\nabla\vec{J} = 0 \quad (33)$$

(i.e. the charge conservation inside the conducting media), coupled with Eq. (16).

For the energy balance, Eq. (21) is still valid, but the source term is due only to ohmic losses:

$$S_q = \sigma \vec{\nabla}\phi \cdot \vec{\nabla}\phi \tag{34}$$

The current collector is in direct contact with one of the electrodes, with the gas, and eventually with the surroundings (depending on the geometry, and, in the case of the planar configuration, if this is the bipolar plate on the top, on the bottom, or inside the stack). In the first case, heat is exchanged for conduction, while in the second and the third for convection. Finally, due to the high temperature, radiation also plays an important role [32–34].

2.4. Electrolyte

As for the current collector, there is no chemical reaction occurring in the electrolyte. Ions flow from one side to the other, thus generating ohmic losses and heat due to the Joule effect. The same equations used for the current collector can be used to describe the electrolyte phenomena. In this case, however, heat is exchanged only for conduction. The equations to be used are here reported for the reader's convenience:

$$\nabla^2 \phi = 0 \tag{35}$$

$$\nabla \vec{J} = 0 \tag{36}$$

$$\vec{J} = -\sigma \nabla \phi \tag{37}$$

$$\frac{\partial Q}{\partial t} + \nabla \vec{Q} + S_q = 0 \tag{38}$$

$$S_q = \sigma \vec{\nabla}\phi \cdot \vec{\nabla}\phi \tag{39}$$

3. Numerical model

3.1. Equations discretization

The governing equations that model an SOFC are highly non-linear and self-coupled, which make it impossible to obtain analytically exact solutions. Therefore, the equations must be solved by discretization thus converting them to a set of numerically solvable algebraic equations.

The appropriate solution algorithm to solve a system of partial differential equations strongly depends on the presence of each term and their combinations.

The three most commonly used computational techniques to discretize a system of partial differential equations are:

- Finite Difference Method (FDM) [35].
- Finite Volumes Method (FVM) [36,37].
- Finite Elements Method (FEM) [38–40].

Each approach allows transforming the continuous problem into a discrete problem with a finite number of degrees of freedom.

The basic idea of the FDM is to replace the individual terms in partial differential equations with finite difference forms at a discrete set of points (the mesh).

In both the FEM and the FVM the spatial domain is divided into a finite number of sub-domains (elements or volumes) and the attention is focused on these sub-domains rather than on the nodes (as it is for the FDM). In the FEM and the FVM, in fact, the integral form of the conservation equations is taken into account and the integration is made over the prescribed finite volumes. It is important to underline that the finite volume over which the integration is made may coincide with a sub-domain of the mesh. Central to FVMs and FEMs is the concept of local conservation of the numerical fluxes. The integration of the convective term of a conservation equation over a finite volume leads, in fact, to the flux of the generic variable through the finite volume boundary surface, by applying the well-known Gauss theorem.

The main difference between a FEM and a FVM is that in the first, a function is assumed for the variation of each variable inside each element while in the latter this function is always equal to 1.

Another important feature of FVMs and FEMs is that they may be used on arbitrary geometries, using structured or unstructured meshes.

As shown above, independently from the numerical method, the spatial continuum is divided into a finite number of discrete cells, and finite time-steps are used for dynamic problems.

In order to perform space discretization, the domain over which the governing equations apply is filled with a predetermined mesh or grid. The mesh is made up of nodes (i.e. grid points) and/or elements at which the physical quantities (i.e. unknowns) are evaluated. Neighboring points are used to calculate derivatives.

Mesh generation is a very complex task for applied problems and many different approaches to it have been developed and are currently under study [41–44].

First of all, computational grids are classified as structured or unstructured meshes, even if each of these classes comprises a broad list of meshing techniques.

The simplest structured mesh is the Cartesian mesh, where nodes are distributed regularly at equal distance from one another. Usually FDMs are applied to structured Cartesian meshes. More generally, a grid is classified as structured when only the physical location (coordinates) of each node must be stored since the identity of neighboring mesh points is known implicitly. This comprises also multiblock structured grid generation schemes (a collection of several structured blocks connected together). The main advantage of structured grids is the simplicity in terms of application, development, computation and visualization. The automatic connectivity information implies that structured grids require the lowest amount of memory for a given mesh size and the related simulation is faster. However, structured grids may represent a severe limitation for practical engineering purposes especially when the geometry is complex and there is a need for high resolution in particular regions of the domain.

In an unstructured mesh each node can have a different number of neighbors and elements have different shapes and sizes.

Therefore, connectivity information must be explicitly defined and stored. The unstructured grid approach, that has gained popularity with the enormous advancements of computer technology, allows handling complex geometries with a lower number of elements and a much easier realisation of local and adaptive grid refinement [44].

A detailed description of mesh generation theory goes beyond the present paper and the reader can refer to literature [41–44]. However, it is important to underline that the accuracy and the stability of any numerical computation are significantly influenced by the particular meshing strategy.

In the case of dynamic (unsteady) problems, even after the space discretization, we still have to solve a set of ordinary differential equations in time. Therefore, the second step is to discretize the temporal continuum. This is usually done by a finite difference approximation with the same properties of an FDM in space. Depending on the instant in which the information is taken, the time-discretization leads to:

- an explicit scheme, when the solution at time step $n+1$ depends only on the known solution at time step n (time-marching solution);
- an implicit scheme, when the time-discretization step leads to a non-linear algebraic system of equations that must be solved to calculate the solution at time $n+1$.

Associated with numerical problems is the concept of stability. A numerical scheme is stable when a solution is reached even with large time-steps (unsteady problems) or iteration steps (algebraic system of equations iteratively solved). Therefore, the size of the time-step or of the iteration-step is dictated by stability requirements. It must be kept in mind that stability does not mean accuracy: an implicit scheme of a dynamic problem is unconditionally stable but the solution obtained with large values of the time step may not be realistic.

3.2. Approaches for the problem solution

According to the specific needs of the model, the equations previously defined can be implemented, formulating some simplifications in the equations themselves or neglecting one or more geometry dimensions. In the following, the formulations of the problem, according to different approaches are briefly presented.

3.2.1. Three-dimensional approach

This approach is used when detailed information on the fuel cell operation is needed. In this case, all the equations given in the previous sections are solved. If the dynamic behavior of the fuel cell is not relevant, the time-dependent terms are neglected, thus the results are relative to the steady state condition. The boundary conditions described in Section 4 need to be implemented.

3.2.2. Two-dimensional approach

In this case, one geometrical dimension is neglected and a 2D section is considered as representative for the entire cell operation. Fig. 4 shows how a micro-tubular SOFC geometry can be reduced in a 2D domain. Thanks to the perfect cell symmetry, the only assumption in this case is that for each angular section, the cell behavior is the same.

For other geometries, a 2D approach prompts to some assumptions and simplifications, causing a reduction in the resulting information. Consider, for example, Fig. 5, where a planar SOFC is depicted. The representative two-dimensional section can be chosen in several ways. In Fig. 5, three cases are identified. In case 1, one section along the cell is chosen. In this case, the section cannot be considered as representative for the entire cell operation. In fact, the gas species are consumed and produced while flowing into the channel. As a result, the current density, the temperature and all the other physical proprieties vary in the x direction. Sometimes a quasi-three-dimensional approach is used by discretizing the cell into a finite number of sections modeled with a two-dimensional approach and dynamically coupling (input of ith section = output of $(i-1)$th section) the resulting two-dimensional models.

Another approach is to choose a section in the xz plane (cases 2 and 3), thus the variation in the x direction can be considered. However, in case 2, the section does not comprise the gas channel, while, in case 3, the current collector is not in direct contact with the electrode. Therefore, the electrical potential of the exter-

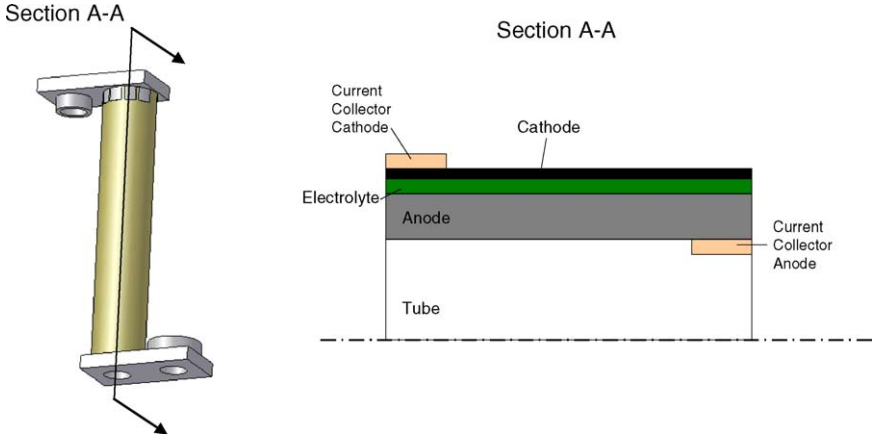

Fig. 4. Simplification of a micro-tubular geometry in 2D.

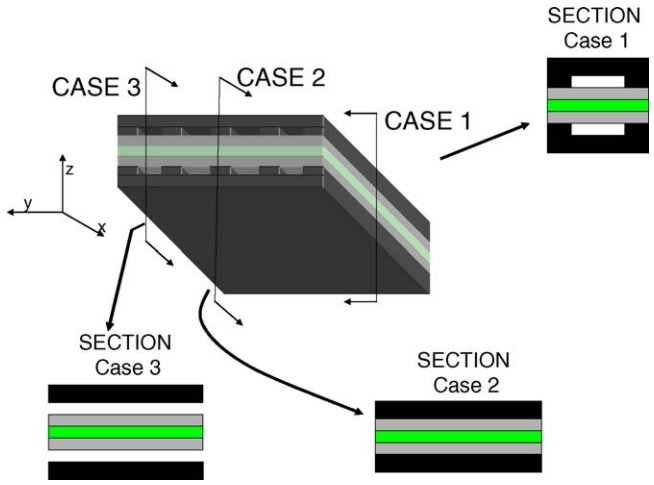

Fig. 5. Possible cross-sections for a 2D representation.

nal electrode boundary is not a constant (contrarily to case 2). Moreover, in both cases 2 and 3, the ohmic resistance variation along the neglected direction needs to be taken into account in the model formulation. In fact, the general expression to evaluate the ohmic resistance is:

$$R_{\text{ohm}} = \frac{1}{\sigma}\frac{t}{S} \tag{40}$$

where t and S are, respectively, the thickness and the section of the conducting medium, where the current passes through. Expression (40) shows that the ohmic resistance is strictly linked to the conductive medium geometry and the current path (i.e. the terms "thickness" and "section"). For this reason, equivalent circuit models for evaluating the equivalent resistance domain are implemented (e.g. [45]). The most complex situation is that of the Siemens–Westinghouse design (Fig. 6). In this configuration, the internal part of the tube constitutes the cathode, while the external is the anode. Single cells are connected to each other by conductive strips inserted to the anode of one cell and touching the cathode of the contiguous single cell. The current path of the cell is shown in the cross-section of the cell. Clearly, it is not easy to determine what t and S are, according to expression (40), thus requiring equivalent circuit models. Bharadwaj et al. [46] developed an analytical model to determine the ohmic polarization of the Siemems–Westinghouse tubular cells. Using a similar approach, in other publications, the authors also computed the ohmic resistance of the novel high power density (HPD) design of Siemens–Westinghouse [47].

Another possibility, not shown in Fig. 5, is to choose the x–y plane (e.g. [48]). However, in this case, there is only one plane (i.e. the x–y itself) representing the entire cell, thus no information on single cell components (electrodes, electrolyte, current collectors) can be directly deduced.

3.2.3. One-dimensional approach

In 1D models only one geometrical dimension is considered and the fuel cell is represented by a line. This is equivalent to make the assumption that the variation of the fluid and the electrical properties along the other two directions is negligible.

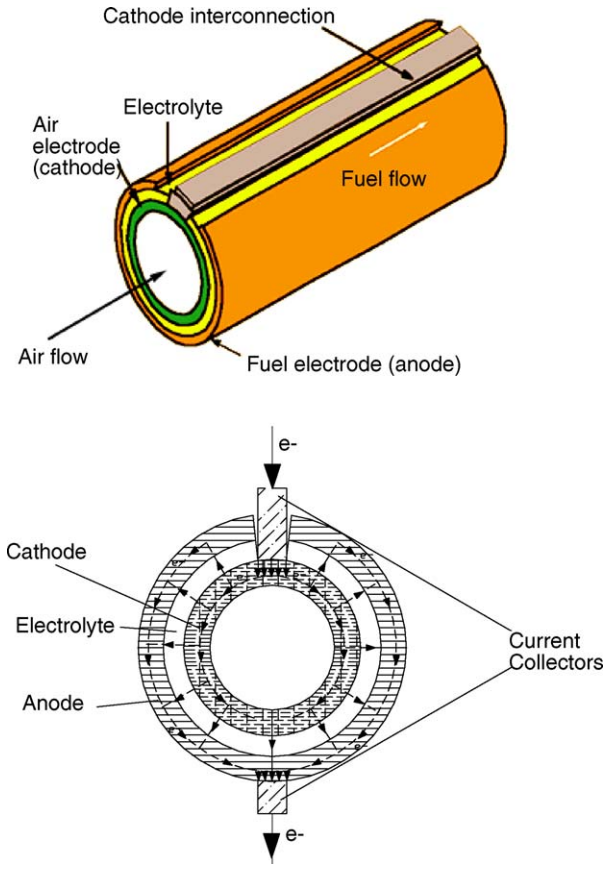

Fig. 6. Siemens–Westinghouse design (top) and relative cross-section (bottom).

As it is for 2D models, reducing a fuel cell into a 1D domain is a non-trivial task and the resulting simplification leads to neglecting important phenomena that must be considered by other means (i.e. concentration losses).

In 1D planar SOFC models the dimension considered is usually determined by the gas flow direction. Therefore, the coordinate varies along a direction parallel to the axes of the gas channels (referring to Fig. 5, x-direction), and this means that cross-flow planar SOFCs cannot be simulated by means of 1D models. By making more simplifying assumptions Standaert et al. [49] have proposed an analytical 1D model for planar molten carbonate fuel cells, later extended to SOFCs by Bove et al. [50].

For tubular SOFCs the kept dimension is usually the tube axis (which coincides with the direction of the fuel and oxidant flow), as in the models presented by Haynes and Wepfer [51], by Ota et al. [52] and by Bove et al. [50], as well as by Li and Suzuki [53] and by Yokoo and Take [54] that extended the 1D analysis to the pre-reformer and the internal reformer following the flow direction.

Gas composition and flow rate in each gas channel are average values of the channels section. In the majority of the 1D models presented in literature a simplified electrochemical model is considered and the fuel cell voltage is calculated by subtracting losses by the ideal (Nernst) potential. The porosity effects of the electrodes (neglected in a 1D model) are considered by means of concentration losses, thus Eqs. (24)–(31) are replaced with a

voltage reduction term (concentration loss), that can be modeled with easy or more sophisticated approaches.

An equivalent electrical circuit must be constructed in order to take into account all the ohmic resistances (also those along the neglected dimensions) along the current path.

This kind of models allows to calculate current density and voltage distribution along the fuel cell length. If heat transfer is taken into account temperature variation along the fuel cell can be calculated.

3.2.4. Zero-dimensional approach

Zero-dimensional models, also called box models, are the simplest ones. The fuel cell is represented by only one box and spatial averaging all dimensions is performed. Thus, spatial variations are not taken into account and one or more transformations (i.e. global mass and energy balances) are considered to define output variables from input ones. In a dynamic simulation, time is the only independent variable.

A zero-dimensional model could be developed to examine the impact of inlet composition, utilization factors and overpotential on the performance of an SOFC in terms of efficiency and characteristic curve. The thermodynamic variables, temperature and pressure, the mass flow rates and the gas composition are assumed to be global values that may change in time (dynamic models) or from input to output values.

However, considering that when the spatial variation of the variables is neglected (i.e. the geometry does not affect directly the performance of the fuel cell) these models are not suitable to performance prediction. More appropriately, zero-dimensional models should be used where attention is not focused on the fuel cell itself but on how the fuel cell affects the performances of the whole system. Two categories of zero-dimensional models are the empirical models (the performances of the fuel cell are already known experimentally) or the so-called "state-of-the-art" components in more complex systems (i.e. combined energy systems).

Box models are usually employed, as thermodynamic models, for the numerical analysis of fuel cell based energy systems (i.e. SOFC/gas turbine hybrid systems and CHP configurations) where the single elements such as compressors, heat exchangers, fuel reformer, partial oxidizers, contaminant removal apparatus, are simulated through independent box models [55,56]. The results of each block are the input data for the next block.

For instance Lunghi and Ubertini [57] integrated a zero-dimensional model of a planar SOFC into a system sequential software (based on Aspen Plus^{TM}) in order to study different configurations of SOFC/GT hybrid systems (Fig. 7 shows one power plant layout studied by Lunghi and Ubertini [57]). The input data to the fuel cell model are gas temperature, pressure, mass flow rate and gas composition. SOFC performances are evaluated through a simplified electrochemistry model:

$$V = V_{rev} - \eta_{ohm} - \eta_{act,a} - \eta_{act,c} - \eta_{con} \tag{41}$$

where the ohmic resistance is estimated considering the resistivity values and the geometry of the cell components and interconnect materials.

The overpotentials due to the activation barriers at the electrodes, η_{act}, are calculated through the Butler–Volmer Eq. (18) by means of a mean current density value.

The concentration polarization losses are expressed as a function of the limiting current, i_l, which is usually taken as a measure of the maximum rate at which a reactant can be supplied to an electrode:

$$\eta_{con,el} = \frac{RT}{2F} \ln\left(1 - \frac{i}{i_l}\right) \tag{42}$$

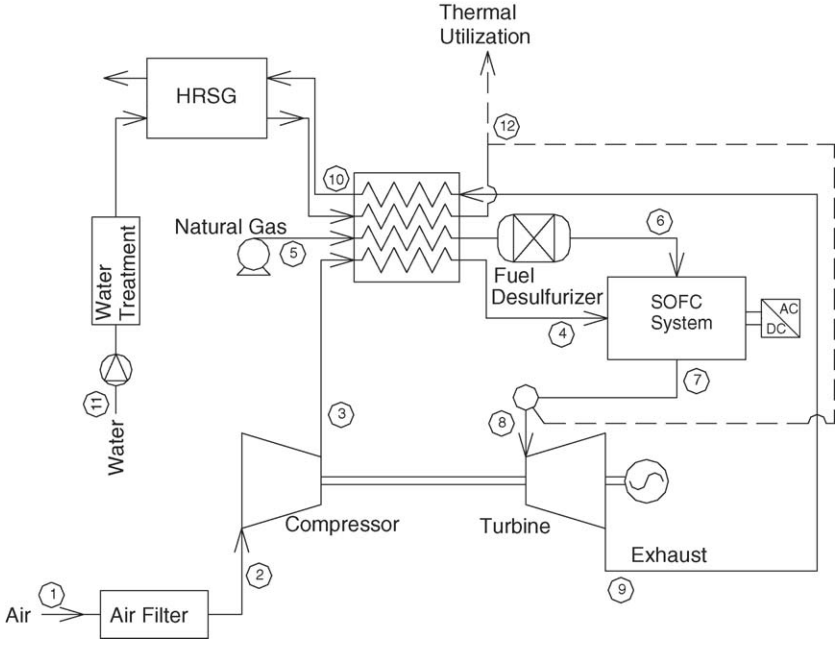

Fig. 7. Low pressure SOFC–GT hybrid plant with steam production [57].

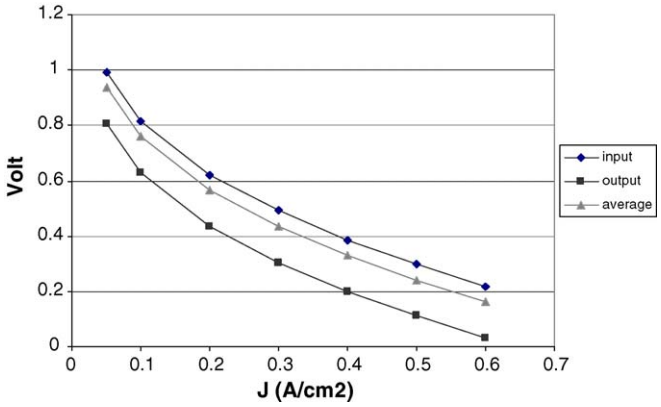

Fig. 8. Variation of the simulated polarization curves if inlet, outlet or an average chemical composition of the gases are considered in a zero-dimensional model [58].

Finally, the thermal behavior of the cell is evaluated through the energy balance of the system assuming one representative temperature for each cell element and reactant gas.

The outputs of this box model are the fuel cell power output and the outlet gas composition and temperature.

In zero-dimensional models it is assumed that the fuel cell is a zero-dimensional space (a point). However, two conditions, inlet and outlet, are present and an ambiguity arises when cell performances are calculated. Cell voltage, in fact, depends on gas concentration and different results are obtained if inlet or outlet gas composition are used. Fig. 8 shows how the characteristic curve of an SOFC changes using inlet, outlet or an average gas concentrations [58].

Fuel cell zero-dimensional models, as the one described above, are usually based on assumptions, parameters and practical information provided in literature or taken from experiments. The objectives of this kind of analyses could be the evaluation of optimal power plant design, configuration, lay-out and components sizing and of the related performances in terms of efficiency and power output. Parametric studies of SOFC based energy systems can be performed in a relatively short time for optimizing the performances and the operation in function of design and operation parameters of the fuel cell (i.e. stack size, utilization factors, cell temperature) and of the other system components.

For instance, Costamagna et al. [55] developed a zero-dimensional model of a SOFC/micro gas turbine (MGT) hybrid system to analyse a SOFC/MGT hybrid system under variable fuel cell and MGT operating conditions, with particular emphasis on the MGT rotational speed. The fuel cell group is a tubular SOFC modeled through macroscopic equations that express the balance between inlet and outlet conditions. The system simulations have been performed on the basis of experimental maps for the compressor and the turbine and of indications from the literature on SOFC and MGT plants. This simplified zero-dimensional approach was used in order to save computational time while maintaining an acceptable accuracy in the overall plant performances evaluation.

As a result they could evaluate the performances of the SOFC/GT energy system under part-load and off-design conditions, by varying a huge quantity of parameters. In particular, Fig. 9 shows the hybrid plant performances, in terms of efficiency versus net non-dimensional power (part-load conditions), at different SOFC air utilization factors and current densities under variable MGT speed. The results show that the possibility of varying the MGT rotational speed allows maintaining high overall system efficiency even at very low load conditions.

This kind of analysis is of fundamental importance to estimate the potential of the hybrid system for distributed energy that is characterized by highly variable electric and thermal loads. Combining the graph shown in Fig. 9 with the load request, in fact, would allow to find the optimal operating parameters for the chosen application.

3.2.5. Multi-dimensional approach

It is a common practice to combine more approaches, especially in complex energy systems as fuel cells. For instance, a

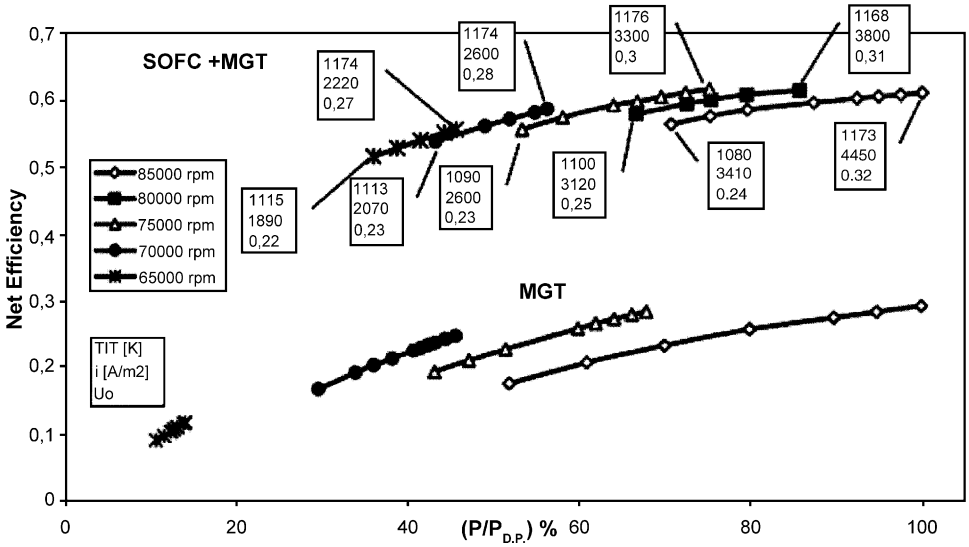

Fig. 9. Part-load performances of a SOFC/MGT hybrid system. MGT stands for micro gas turbine and $P/P_{D,P}$ stands for net non-dimensional power [55].

zero-dimensional model may be used to estimate initial values for a three-dimensional simulation. Moreover a one-dimensional approach can be used to model the flow field in the gas channels together with a two-dimensional model of the temperature and the current paths at the electrodes.

Multi-dimensional models could be considered as modular softwares where the different components could be simulated through 0D, 1D, 2D or even 3D models.

4. Boundary conditions (internal and external)

The accuracy of a modeling technique prediction is highly sensitive to the specification of the initial and the boundary conditions, which usually represents the major part of the computational effort. In a few words, boundary conditions are the mathematical description of the different situations that produce different results within the same physical system (same governing equations). A proper specification of the boundary conditions is necessary to allow the calculation. Once boundary conditions are defined, the so-called "properly-posed problem" is reached. Moreover, it must be noted that in modeling an SOFC there are various intrinsically coupled flow, thermal, chemical and electrochemical phenomena and different physical systems to be modeled. This means that the definition of the boundary conditions incorporates both external boundary conditions and interface boundary conditions.

The type of partial differential equations and the discretization approach determine the form of the boundary conditions, that are usually classified either in terms of their mathematical description or in terms of the physical type of the boundary.

For steady state problems the following two types of spatial boundary conditions are identified:

- Dirichlet boundary condition, when the generic variable on the boundary assumes a known and constant value;
- Neuman boundary condition, when the derivatives of the generic variable on the boundary are known and this yields an extra equation.

Physical boundary conditions depend on the specific problem to be solved.

In the fluid problem within the gas channels the following boundary conditions are observed:

- stationary solid walls (sidewalls) where the velocity components vanish at the walls and the heat flux must be defined;
- interface between the gas channel and the porous media where mass and energy crosses the boundary surface in either direction; these conditions are therefore usually given imposing the continuity of mass and energy fluxes;
- open flows (inlet and outlet) where the fluid enters or leaves the domain; fluid velocity or pressure values together with, or the mass flow rate should be defined as well as the specific enthalpy for the energy equation; the initial molar or mass fraction of the different species must be also imposed at inlet.

In the following the possible boundary conditions, for each previously defined equation, are given.

4.1. Channels flow

In order to solve Eqs. (6), (10) and (12), a number of uncoupled conditions equal to the number of unknowns need to be specified at the boundaries (boundary conditions). These are the mass fractions Y_i (continuity equation), the fluid temperature T (energy equation) and a characteristic of the flow field (momentum equation), i.e. u or P. Taking as a reference the case of Fig. 1 (planar configuration), the molar fraction needs to be specified at the inlet, while at the channel boundaries, there is no variation. At the electrode/channel flow interface and at the outlet, the continuity is imposed. The velocity of the fluid is zero at the channel walls, while it is specified at the inlet and outlet. Alternatively, it can be convenient to specify (usually at the outlet) the pressure.

4.2. Electrodes

According to the schematization of Fig. 1, the electrodes are in contact with the electrolyte on one side, and with the gas and the current collector on the other side. Although the tubular configuration presents a different geometry, it is always possible to identify these three boundary faces [15]. For the sake of simplicity, the planar configuration is taken as reference, and the electrode domain is reported in Fig. 10; however, in complete analogy, similar boundary conditions can be provided for the tubular or monolithic configuration.

Surfaces S1, S2, S4 and the other perimeteral surface not represented in Fig. 10 (because hidden) are insulated, thus the boundary conditions for the electrical, thermal and mass transport problems are:

$$\vec{J} \cdot \vec{n} = 0 \tag{43}$$

$$\vec{Q} \cdot \vec{n} = -\lambda \vec{\nabla} T \cdot \vec{n} = 0 \tag{44}$$

$$\nabla \vec{m}_i \cdot \vec{n} = 0 \tag{45}$$

Alternatively, an estimation of the heat, mass and current loss can be provided. The estimation of these quantities are usually affected by a large uncertainty degree, thus the ideal case is usually considered.

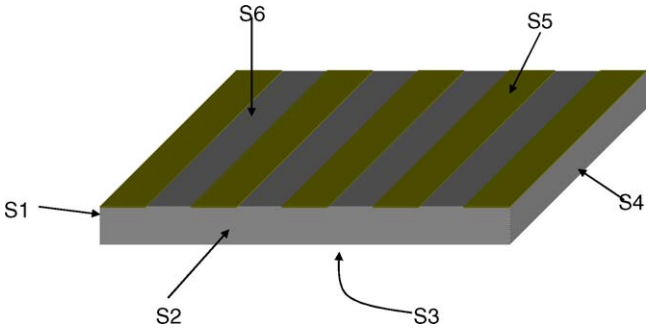

Fig. 10. Schematic representation of the electrode.

Surface S3 represents the boundary between the electrode and the electrolyte. As mentioned in Section 2.2, since the TPB is usually very thin and close to the electrode-interface boundary, the TPB can be assimilated with surface S3. Eqs. (17), (20), (22) and (25) reduce, respectively to:

$$\nabla \vec{J} = 0 \tag{46}$$

$$\nabla^2 \phi = 0 \tag{47}$$

$$S_q = \sigma \vec{\nabla}\phi \cdot \vec{\nabla}\phi \tag{48}$$

$$\omega_i = 0 \tag{49}$$

In this case, the electrochemical reactions (3) and (4) are considered to occur at boundary S3, thus the boundary condition for the electrical problem is provided by Eq. (18) that are here reported for the reader's convenience:

$$\vec{J} \cdot \vec{n} = j_0 \left[\exp\left(\frac{\alpha_1 \eta_{act}}{RT}\right) - \exp\left(\frac{\alpha_2 \eta_{act}}{RT}\right) \right] \tag{50}$$

The condition for the thermal problem is:

$$\vec{Q} \cdot \vec{n} = \frac{J}{2F} T\Delta S + J\eta_{act} \tag{51}$$

while, for the mass transport, the conditions are:

$$\vec{m}_{H_2} \cdot \vec{n} = -\frac{\vec{J} \cdot \vec{n}}{2F} M_{H_2} \tag{52}$$

$$\vec{m}_{H_2O} \cdot \vec{n} = \frac{\vec{J} \cdot \vec{n}}{2F} M_{H_2O} \tag{53}$$

$$\vec{m}_{O_2} \cdot \vec{n} = -\frac{\vec{J} \cdot \vec{n}}{4F} M_{O_2} \tag{54}$$

In expressions (52)–(54), the symbol M_i represents the molecular weight of the ith species. Expressions (52) and (53) are referred to the anode, while expression (54) to the cathode.

Surface S5 is the boundary between the current collector and the electrode. The following conditions are applied:

$$\vec{J} \cdot \vec{n} = \left(\vec{J} \cdot \vec{n}\right)_{\text{interconnect}} \tag{55}$$

$$\vec{Q} \cdot \vec{n} = \left(\vec{Q} \cdot \vec{n}\right)_{\text{interconnect}} \tag{56}$$

$$\vec{m}_i \cdot \vec{n} = 0 \tag{57}$$

The first two expressions state the current and heat flux continuity, while the third states the mass insulation, due to the current collector.

Finally, surface S6 is in direct contact with the gas. In this case there is a mass continuity with the channel flow, insulation for the electric current, and a heat flux due to convection with the gas and radiation from the gas channel walls:

$$\vec{J} \cdot \vec{n} = 0 \tag{58}$$

$$\vec{Q} \cdot \vec{n} = h(T_{S6} - T_{gas}) + Q_{\text{rad-surf}} \tag{59}$$

$$\vec{m}_i \cdot \vec{n} = (\vec{m}_i \cdot \vec{n})_{\text{channel flow}} \tag{60}$$

In expression (59), h is the convective heat transfer coefficient between the gas flow and the electrode, and $Q_{\text{rad-surf}}$ is the radiation heat transferred between S6 and any other visible surface. Murthy and Fedorov [33] noted that the surface-to-surface approach (as that of relation (59)) could lead to some temperature prediction mistakes. More accurate results can be expected considering the absorption, emission or scattering in the media.

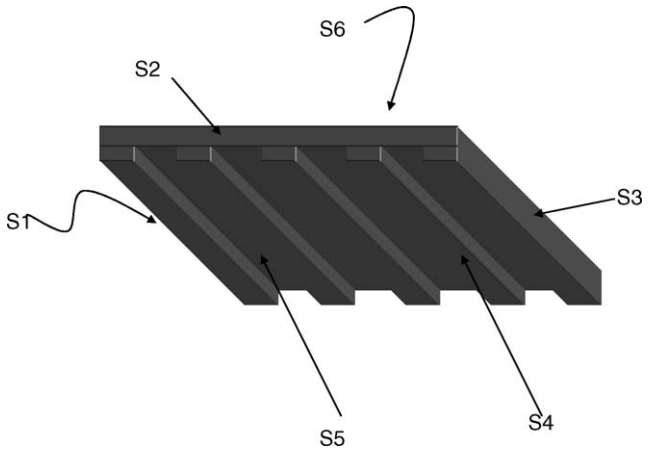

Fig. 11. Current collector/gas channel of a flat planar SOFC.

4.3. Current collectors

Fig. 11 schematically represents the current collector of a planar SOFC. The surfaces that are thermally and electrically insulated are S1, S2, S3 and forth perimeteral face (not indicated Fig. 11). For these faces, the following conditions apply:

$$\vec{J} \cdot \vec{n} = 0 \tag{61}$$

$$\vec{Q} \cdot \vec{n} = -\lambda \vec{\nabla} T \cdot \vec{n} = 0 \tag{62}$$

Surface S5 is electrically insulated, thus expression (61) applies, but convective and radiation heat transfer need to be considered.

$$\vec{Q} \cdot \vec{n} = h(T_{S5} - T_{gas}) + Q_{\text{rad-surf}} \tag{63}$$

For surface S4, the continuity conditions needs to be applied:

$$\vec{J} \cdot \vec{n} = \left(\vec{J} \cdot \vec{n}\right)_{\text{interconnect}} \tag{64}$$

$$\vec{Q} \cdot \vec{n} = \left(\vec{Q} \cdot \vec{n}\right)_{\text{electrode}} \tag{65}$$

Similarly to relation (64) and (65) the continuity conditions for boundary S6 (hidden in Fig. 11), are applied.

4.4. Electrolyte

Referring to Fig. 1, the electrolyte can be regarded as a parallelepiped, where the surfaces constituting the perimeter are insulated:

$$\vec{J} \cdot \vec{n} = 0 \tag{66}$$

$$\vec{Q} \cdot \vec{n} = -\lambda \vec{\nabla} T \cdot \vec{n} = 0 \tag{67}$$

For the surfaces at the top and the bottom, continuity with the two electrodes needs to be expressed.

$$\vec{Q} \cdot \vec{n} = \left(\vec{Q} \cdot \vec{n}\right)_{\text{electrode}} \tag{68}$$

$$\vec{J} \cdot \vec{n} = 0.5\left(\vec{J} \cdot \vec{n}\right)_{\text{electrode}} \tag{69}$$

The term 0.5 in Eq. (69) takes into account that, as stated in Eq. (4), every two electrons released (reacting) at the anode (cathode), one O^{2-} ion flows through the electrolyte. As a reminder, Eqs. (35)–(37) assume that the ionic current follows the ohmic law.

5. Validation

Since the numerical result of a computation is only an approximation of real life and considering that convergence is not a sufficient condition to stability, a necessary step in the development of a computational model is validation. Validation is performed through the comparison between numerical results and experimental data to establish the range of validity and the accuracy of the code. Blind acceptance of computed results are not a good basis to make engineering decisions involving financial and time schedule risks. However, it is important to underline that even a validation against many and the most complex problems cannot prove that the model is totally error-free.

If poor agreement is found between experiments and computations, the task is to understand error sources both in the code and in the measuring system: the input data may involve too much guess-work or imprecision; the available computer power may be too small for high numerical accuracy; the scientific knowledge base may be inadequate.

6. Results

In the present section, results obtained from the approaches described in Section 3.2 are provided.

6.1. Three-dimensional approach

Three-dimensional models, coupling and solving electrical, fluid dynamic, chemical and thermal problems are very complex, time consuming and can require strong numerical simulation expertise and hardware. For this reason 3D models usually found in the literature model only some of the above problems, and neglect others. However, due to the recent improvements of the simulation tools (hardware and software), some authors have implemented all the equations (even if with some simplified assumptions). Fig. 12 shows the mesh of a five channels, cross-flow, electrolyte supported planar SOFC [59]. The related current density distribution is depicted in Fig. 13. The details of the results and the relevant amount of information that can be deducted from this analysis is clear from Fig. 13. Such results can be obtained for all the other physical characteristics considered in the model, such as temperature, velocity distribution, concentration distribution, electrical potential, etc.

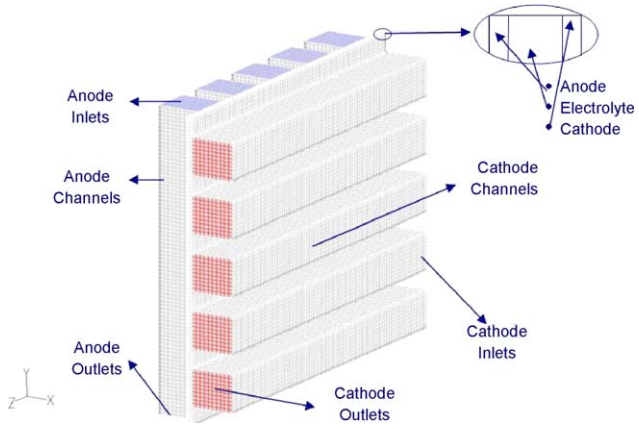

Fig. 12. Mesh of a five channels, cross-flow, electrolyte-supported SOFC [59].

6.2. Two-dimensional approach

As explained in Section 3.2, there are different approaches to simplify a domain from 3D to 2D. In the present section, as an example, the case of a micro-tubular SOFC is illustrated. Fig. 4 depicts the micro-tubular SOFC, modeled by Bove and Sammes [14]. In this configuration, the current collectors are placed at the two ends of the tube, thus representing two caps for the tube. One cap touches the outer part of the tube (cathode) and the other the inner part (anode). Due to the circular symmetry of the cell, modeling the fuel cell in a 2D environment, does not lead to any loss of information. Results for the current path in the cell are depicted in Fig. 14 [14]. Please note that since the electrolyte and cathode are much thinner than the anode, only the current path trough the anode is visible in the figure. However, since the anode conductivity is much higher than that of the electrolyte, ions migration through the electrolyte is limited to the tube part very close to the cathodic current collector (left hand side of Fig. 14). As a consequence, even electrons migration

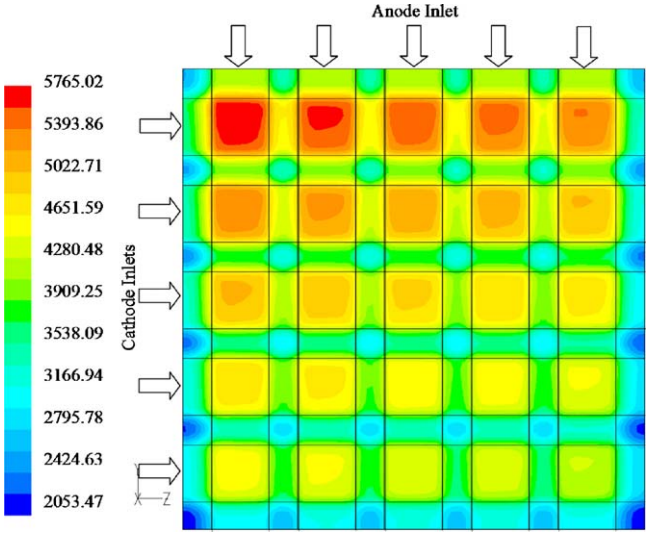

Fig. 13. Current density distribution ($A\,m^{-2}$) in a planar solid oxide fuel cell [59].

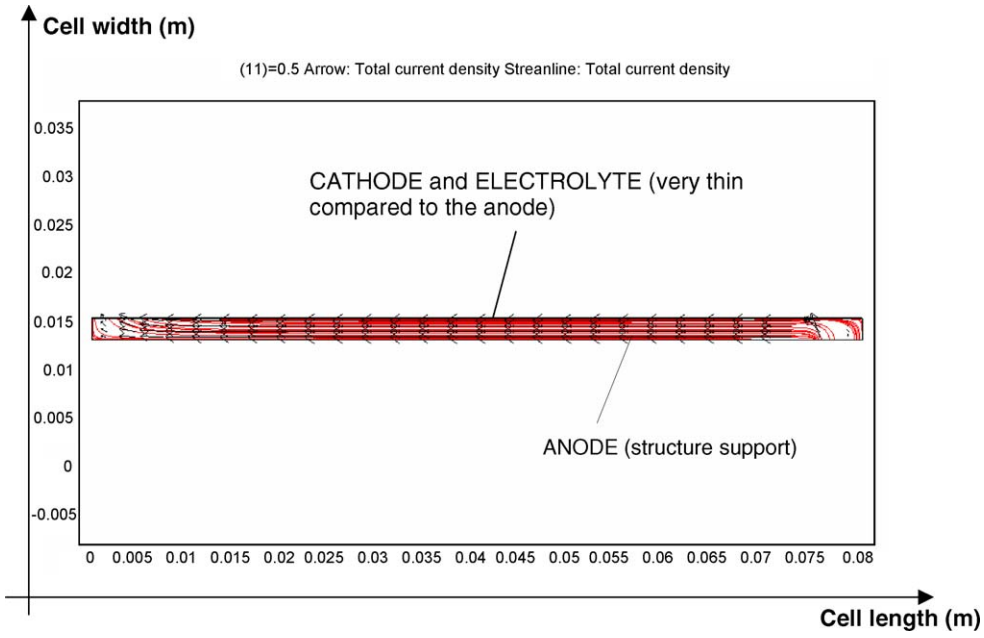

Fig. 14. Current path in a micro-tubular SOFC, with the current collectors at the two tube's ends [14].

along the cathode length is negligible. For more details about the current path in this configuration, please refer to [14]. The model allows to fully understand the reason for a poor performance, when current collectors are placed in this configuration. The current path, in fact, is mainly along the cell, thus a high ohmic resistance is generated. In the same study, Bove and Sammes [14] also analyzed the performance achievable if, together with the two caps, the current is collected using a wire wrapped around (internally and externally) the cell. The results for the current density path is depicted in Fig. 15. Comparing Figs. 14 and 15, it is clear how a reliable model can help the research in designing single components, as well single cells.

6.3. One-dimensional approach

As fully explained in Section 3.2, the use of a one-dimensional approach implies to neglect those phenomena occurring in the two directions not considered in the model. More evolved models, however, even if consider the gas moving in one direction, take into account the interaction between different layers that constitute the single cell. Fig. 16 shows how Haynes and Wepfer simplified a Siemens–Westinghouse tubular cells [60], and the related results for the variation of the fluid temperature along the cell are represented in Fig. 17.

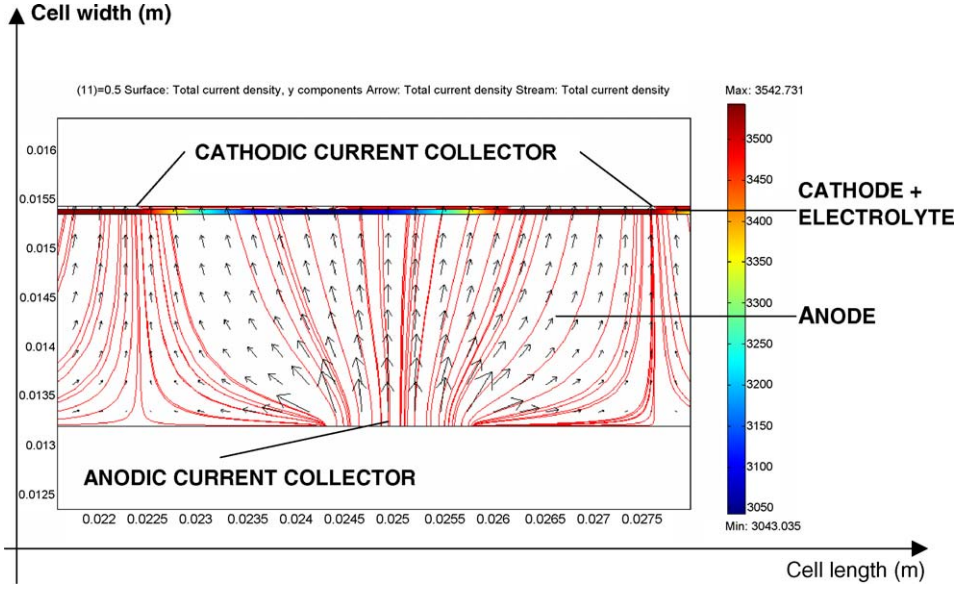

Fig. 15. Results for current density distribution in a micro-tubular SOFC with wires wrapped around the tube [14].

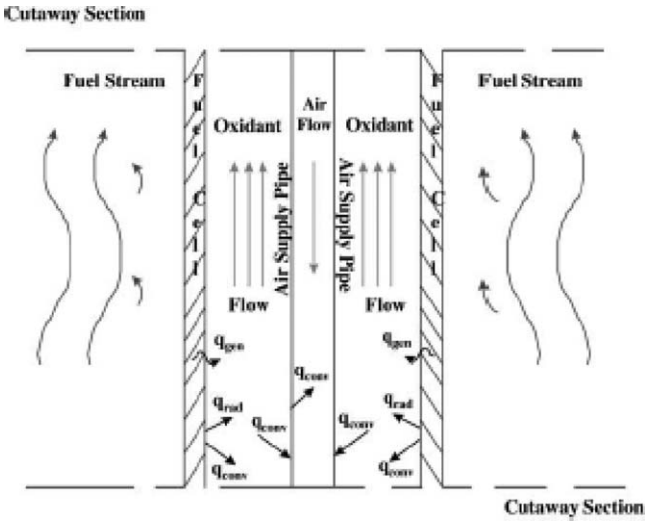

Fig. 16. Schematic representation in 1D of the Siemens–Westinghouse tubular cell [60].

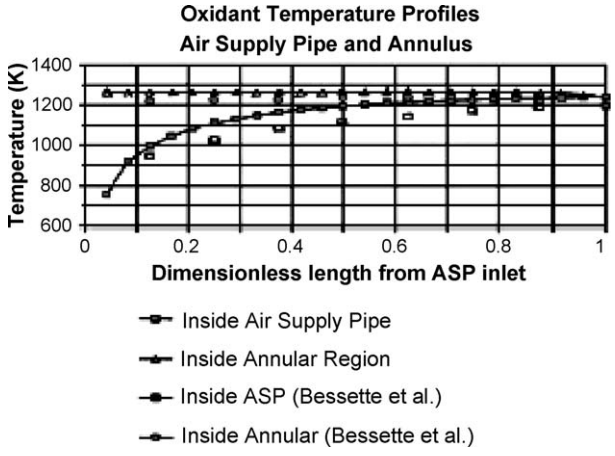

Fig. 17. Fluid temperature profile inside a Siemens–Westinghouse tubular cell [60].

6.4. Zero-dimensional approach

Results for zero-dimensional models can provide only information on the overall performance, like for example, chemical composition and temperature of inlet and outlet gas, cell voltage, power density and efficiency. Typically, the information required from these kind of models are the polarization curve, the power density and the efficiency variations with the current density variation. Fig. 18 represents the polarization curve for a tubular Siemens–Westinghouse SOFC, operating at different temperatures.

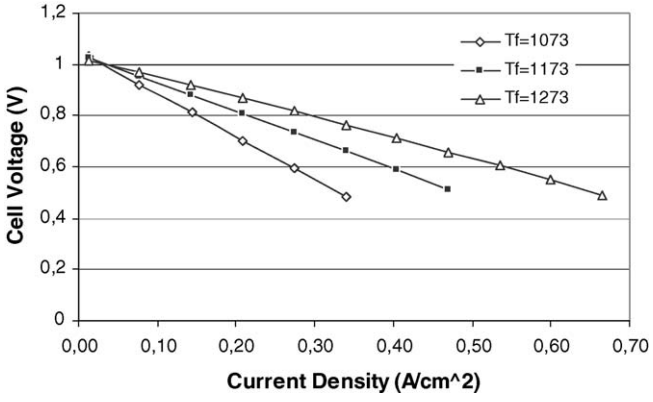

Fig. 18. Polarization curve of a tubular Siemens–Westinghouse single cell operating at different temperature, obtained through a zero-dimensional model.

7. Conclusions

This paper focuses on the development of a detailed numerical model of an SOFC. A complete analysis of the phenomena acting in solid oxide fuel cells is presented and the three-dimensional mathematical model of each element of the SOFC, built on the basis of conservation and constitutive laws, is written. The mathematical model is a complete, 3D and time-dependent model independent of the fuel cell geometry (i.e. planar and tubular, monolithic) and the modeling approach (i.e. time-dependent, 3D, 2D). Then the discretization to produce a numerical analogue of the equations is discussed. The boundary conditions, that strongly influence the accuracy of the model and usually represent a significant part of the computational effort, necessary to reach a properly-posed problem are shown.

Finally, a literature review is conducted. Some results from the models previously developed by the authors or found in the literature survey are presented. Each of them can be reviewed as a simplified version of the model presented in the present paper. The simplified assumptions and the related omissions that each of those approaches imply are also analyzed.

References

[1] U.G. Bossel, Facts & Figures. Final International Energy Agency Report, Berne, April 1992.
[2] E. Achenbach, Three-dimensional and time dependent simulation of a planar solid oxide fuel cell stack, J. Power Sources 49 (1994) 333–348.
[3] N.F. Bessette, W.J. Wepfer, J. Winnick, A mathematic model of a solid oxide fuel cell, J. Electrochem. Soc. 142 (11) (1995) 3792–3800.
[4] J.R. Ferguson. SOFC two dimensional “unit cell” modeling, SOFC Stack Design Tool, International Energy Agency Final Report, 1992.
[5] L. Petruzzi, S. Cocchi, F. Fineschi, Global thermo-electrochemical model for SOFC systems design and engineering, J. Power Sources 118 (2003) 96–107.
[6] C. Hirsch, Numerical Computation of Internal and External Flows, John Wiley & Sons, 1992.
[7] M.B. Abbott, D.R. Basco, Computational Fluid Dynamics: An Introduction for Engineers, Longman Scientific & Technical/Wiley, Harlow, Essex, England/New York, NY, 1989.
[8] S.V. Patankar, Numerical Heat Transfer and Fluid Flow, Hemisphere Publishing Corporation, 1980.
[9] J.H. Ferziger, M. Peric, Computational Methods for Fluid Dynamics, Springer-Verlag, 1995.
[10] R.B. Bird, W.E. Steward, E.N. Lightfoot, Transport Phenomena, J. Wiley & Sons, New York, 1960.
[11] M.M.A. Khaleel, Z. Lin, P. Singh, W. Surdoval, D. Collin, A finite element analysis modeling tool for solid oxide fuel cell development: coupled electrochemistry, thermal and flow analysis in MARC, J. Power Sources 130 (2004) 136–148.
[12] J.B. Goodenough, Oxide components for the solid oxide fuel cell, in: N. Orlovskaya, N. Browing (Eds.), Mixed Ionic Electronic Conductive Perovskites for Advanced Energy Systems, NATO Science Series, Kluwer Academia Publisher, 2004.

[13] R.S. Gemmen, C.D. Johnson, Effect of load transient on SOFC operation – current reversal on loss of load, J. Power Sources 144 (2005) 152–164.
[14] R. Bove, N.M. Sammes, The effect of current collectors configuration on the performance of a tubular SOFC, in: Proceedings of the Ninth International Symposium on Solid Oxide Fuel Cells (SOFC IX), Quebec City, Canada, May 15–20, 2005.
[15] R. Bove. Technical and environmental evaluation of high temperature fuel cells through numerical simulations and in field tests, Ph.D. Thesis, University of Perugia, Italy, 2004.
[16] G.F. Froment, M. Bishoff, Chemical Reactors Analysis and Design, J. Wiley & Sons, New York, 1990.
[17] J. Bear, J.M. Buchlin, Modeling and Application of Transport Phenomena in Porous Media, Kluwer Academic Publishers, Boston, MA, 1991.
[18] J. Bear, Dynamics of Fluids in Porous Media, Dover Publications, Inc., New York, 1972.
[19] R. Suwanwarangkul, E. Croiset, M.W. Fowler, P.L. Douglas, E. Entchev, M.A. Douglas, Performance comparison of Fick's, dusty-gas and Stefan–Maxwell models to predict the concentration overpotential of a SOFC anode, J. Power Sources 122 (2003) 9–18.
[20] S. Campanari, P. Iora, Definition and sensitivity analysis of a finite volume SOFC model for a tubular cell geometry, J. Power Sources 132 (May (1–2)) (2004) 113–126.
[21] S.H. Chan, K.A. Khor, Z.T. Xia, A complete polarization model of a solid oxide fuel cell and its sensitivity to the change of cell components thickness, J. Power Sources 93 (2001) 130–140.
[22] J.R. Ferguson, J.M. Fiard, Herbin, Three-dimensional numerical simulation for various geometries of solid oxide fuel cells, J. Power Sources 58 (1996) 109–122.
[23] S.B. Beale, Calculation precedure for mass transfer in fuel cells, J. Power Sources 128 (2004) 185–192.
[24] J.W. Kim, A.V. Virkar, K.Z. Fung, K. Metha, S.C. Singhal, Polarization effects in intermediate temperature, anode-supported solid oxide fuel cells, J. Electrochem. Soc. 146 (1) (1999) 69–78.
[25] J.J. Hwang, C.K. Chen, D.Y. Lai, Computational analysis of species transport and electrochemical characteristics of a MOLB-type SOFC, J. Power Sources 140 (2005) 235–242.
[26] N. Autissier, D. Larrain, J. Van herle, D. Favrat, CFD simulation tool for solid oxide fuel cells, J. Power Sources 131 (2004) 313–319.
[27] M. Iwata, T. Hikosaka, M. Morita, T. Iwanari, K. Ito, K. Onda, Y. Esaki, Y. Sakaki, S. Nagata, Performance analysis of planar-type unit SOFC considerino current and temperature distribution, J. Power Sources 132 (2000) 297–308.
[28] M. Roos, E. Batawi, U. Harnisch, Th. Hocker, Efficient simulation of fuel cell stacks with the volume averaging method, J. Power Sources 118 (2003) 86–95.
[29] J.W. Veldsink, R.M.J. van Damme, G.F. Versteeg, W.P.M. van Swaaij, The use of the dusty-gas model for the description of transport with chemical reaction in porous media, Chem. Eng. J. Biochem. Eng. 57 (1995) 115–125.
[30] H. Yakabe, M. Hishinuma, M. Uratani, Y. Matsuzaki, I. Yasuda, Evaluation and modeling of performance of anode-supported solid oxide fuel cell, J. Power Sources 86 (2000) 423–431.
[31] W. Lehnert, J. Meusinger, F. Thom, Modelling of gas transport phenomena in SOFC anodes, J. Power Sources 87 (2000) 57–63.
[32] A.C. Burt, I.B. Celik, R.S. Gemmen, A.V. Smirnov, Influence of radiative heat transfer on variation of cell voltage within a stack, in: Proceedings of the 1st International Conference on Fuel Cell Science, Engineering and Technology, Rochester, NY, April 21–23, 2003.
[33] S. Murthy, G. Federov, Radiation heat transfer analysis of the monolith type solid oxide fuel cell, J. Power Sources 124 (2) (2003) 453–458.
[34] N.F. Bessette, W.J. Wepfer, Prediction of on-design and off-design performance for a solid oxide fuel cell power module, Energy Convers. Manage. 37 (3) (1996) 281–293.
[35] G.D. Smith, Numerical Solution of Partial Differential Equations: Finite Difference Methods, third ed., Claredon Press, Oxford, 1985.
[36] H.K. Versteeg, W. Malalasekera, An Introduction to Computational Fluid Dynamics: The Finite Volume Method, Addison Wesley Longman, Ltd., Harlow, England, 1995.
[37] R. Eymard, T. Gallouet, R. Herbin, in: P.G. Ciarlet, J.L. Lions (Eds.), Finite Volume Methods, Handbook of Numerical Analysis, vol. VII, 2000, pp. 713–1020 (North Holland).
[38] O.C. Zienkiewicz, R. Taylor, The Finite Element Method: Volumes 1, 2 & 3, fifth ed., Elsevier, Butterworth–Heinemann, 2000.
[39] J.N. Reddy, An Introduction to the Finite Element Method, McGraw-Hill, 1993.
[40] K.J. Bathe, Finite Element Procedures, Prentice Hall, 1996.
[41] J.F. Thompson, Z.U.A. Warsi, C.W. Mastin, Numerical Grid Generation, Foundations and Applications, Amsterdam, North Holland, 1985.
[42] J.F. Thompson, B. Soni, N. Weatherill (Eds.), Handbook of Grid Generation, CRC Press, 1998.
[43] V.D. Liseikin, Grid Generation Methods, Springer, 1999.
[44] S.J. Owen, M.S. Shephard (Eds.), Trends in unstructured mesh generation, Int. J. Numerical Methods Eng. vol. 58 (2) (2003) (Special issue).
[45] U.G. Bossel. Performance potentials of solid oxide fuel cell configurations. EPRI Final Report TR-101109, 1992.
[46] A. Bharadwaj, D.H. Archer, E.S. Rubin, Modeling the performance of a tubular solid oxide fuel cell, J. Fuel Cell Sci. Technol. 2 (1) (2005) 38–44.
[47] A. Bharadwaj, D.H. Archer, E.S. Rubin, Modeling the performance of flattened tubular solid oxide fuel cell, J. Fuel Cell Sci. Technol. 2 (1) (2005) 52–59.
[48] E. Arato, P. Costa, Mathematical modeling of monolithic SOFC. SOFC Stack Design Tool, International Energy Agency Final Report, 1992.
[49] F. Standaert, K. Hemmes, N. Woudstra, Analytical fuel cell modeling, J. Power Sources 63 (2) (1996) 221–234.
[50] R. Bove, P. Lunghi, N.M. Sammes, SOFC mathematic model for systems simulations–Part 2: definition of an analytical model, Int. J. Hydrogen Energy 30 (2) (2005) 189–200.
[51] C. Haynes, W.J. Wepfer, Design for power' of a commercial grade tubular solid oxide fuel cell, Energy Convers. Manage. 41 (2000) 1123–1139.
[52] T. Ota, M. Koyama, C. Wen, K. Yamada, H. Takahashi, Object-based modeling of SOFC system: dynamic behavior of micro-tube SOFC, J. Power Sources 118 (1–2) (2003) 430–439.
[53] P.W. Li, K. Suzuki, Numerical modeling and performance study of a tubular SOFC, J. Electrochem. Soc. 151 (4) (2004) A548–A557.
[54] M. Yokoo, T. Take, Simulation analysis of a system combining solid oxide and polymer electrolyte fuel cells, J. Power Sources 137 (2) (2004) 206–215.
[55] P. Costamagna, L. Magistri, A.F. Massardo, Design and part-load performance of a hybrid system based on a solid oxide fuel cell reactor and a micro gas turbine, J. Power Sources 96 (2) (2001) 352–368.
[56] R. Bove, N.M. Sammes, Behavior of an SOFC System for small stationary applications under full and partial load operation, in: Proceedings of the 6th European Solid Oxide Fuel Cell Forum, Lucerne, Switzerland, 28 June–2 July, 2004.
[57] P. Lunghi, U. Ubertini, Solid oxide fuel cells and regenerated gas turbines hybrid systems: a feasible solution for future ultra high efficiency power plants, in: Proceedings of the Seventh International Symposium on Solid Oxide Fuel Cells (SOFC-VII), Tsukuba, Ibaraki, Japan, 2001, pp. 254–264.
[58] R. Bove, P. Lunghi, N. Sammes, SOFC Mathematic Model for system simulation. Part one: from a micro-detailed to a macro-black-box model, Int. J. Hydrogen Energy 30 (2) (2005) 181–187.
[59] U. Pasaoguillari, C.-Y. Wang, Computational fluid dynamics modeling of solid oxide fuel cells, in: Proceedings of the Eighth International Symposium on Solid Oxide Fuel Cells (SOFC VIII), Paris, France, April 27–May 2, 2003.
[60] C. Haynes, W.J. Wepfer, Characterizing heat transfer within a commercial-grade tubular solid oxide fuel cell for enhanced thermal management, Int. J. Hydrogen Energy 26 (2001) 369–379.